

# Determination of the complex dielectric constant of an epithelial cell monolayer in the terahertz region

Cite as: Appl. Phys. Lett. **102**, 053702 (2013); <https://doi.org/10.1063/1.4790392>

Submitted: 01 November 2012 • Accepted: 22 January 2013 • Published Online: 05 February 2013

K. Shiraga, Y. Ogawa, T. Suzuki, et al.



View Online



Export Citation



CrossMark

## ARTICLES YOU MAY BE INTERESTED IN

[Hydration state inside HeLa cell monolayer investigated with terahertz spectroscopy](#)

Applied Physics Letters **106**, 253701 (2015); <https://doi.org/10.1063/1.4922918>

[Tutorial: An introduction to terahertz time domain spectroscopy \(THz-TDS\)](#)

Journal of Applied Physics **124**, 231101 (2018); <https://doi.org/10.1063/1.5047659>

[Temperature dependent optical and dielectric properties of liquid water studied by terahertz time-domain spectroscopy](#)

AIP Advances **9**, 035346 (2019); <https://doi.org/10.1063/1.5082841>

Lock-in Amplifiers  
up to 600 MHz



Zurich  
Instruments



## Determination of the complex dielectric constant of an epithelial cell monolayer in the terahertz region

K. Shiraga,<sup>1</sup> Y. Ogawa,<sup>1,a)</sup> T. Suzuki,<sup>1</sup> N. Kondo,<sup>1</sup> A. Irisawa,<sup>2</sup> and M. Imamura<sup>2</sup>

<sup>1</sup>Graduate School of Agriculture, Kyoto University, Kyoto 606-8502, Japan

<sup>2</sup>ADVANTEST Corporation, Sendai 989-3124, Japan

(Received 1 November 2012; accepted 22 January 2013; published online 5 February 2013)

We present a method to determine the complex dielectric constant of a cell monolayer using terahertz time-domain attenuated total reflection spectroscopy combined with a two-interface model. The imaginary part of the dielectric constant of the cell monolayer shows a lower absorption of slow relaxation mode than that of the liquid medium. This result allows us to estimate the intracellular water dynamics on a picosecond time scale, and the existence of weakly hydrated water molecules inside the cell monolayer was indicated. This method will provide a perspective to investigate the intracellular water dynamics in detail. © 2013 American Institute of Physics. [<http://dx.doi.org/10.1063/1.4790392>]

Development of gene technologies and molecular biology has allowed elucidation of various cell functions, especially at the biological macromolecule and organelle level.<sup>1</sup> The results from these studies suggest that within intracellular systems, interactions are complicated and regulated by water molecules. These water molecules both the biological molecules, acting as an essential element to support the reactivity of the biological molecules, and for their conformations and functions to be stabilized. It is known that water molecules near the surface of biomolecules (“biological water”) have significantly different properties to that of bulk water.<sup>2,3</sup> The dynamical changes in biological water tied up with these small conformational transitions in biological macromolecules affect the fluidity and activity of the intracellular environment.<sup>4</sup>

Dielectric spectroscopy,<sup>5</sup> nuclear magnetic resonance (NMR),<sup>6</sup> and quasi-elastic neutron scattering (QENS) spectroscopy<sup>7</sup> have been used to investigate intracellular water dynamics. The target of these intensive studies was mainly with cell suspensions or unicellular organisms like *E. coli*. These conventional techniques demonstrate just how different the nature of the intracellular water is compared to bulk water, up to a sub-nanosecond timescale. They also confirm the existence of biological water directly bound to the biological macromolecules.

Nevertheless, when the average distance between biological macromolecules inside cells is considered at 20 Å,<sup>8</sup> 10 water molecules (with a diameter  $\sim 2$  Å) are estimated to fit between these molecules.<sup>9</sup> The dynamics of these water molecules, though not directly bound to the macromolecule (hereafter referred to as global hydration), are nevertheless weakly perturbed by solutes. Due to a lack of appropriate methods though, it has yet to be investigated. This is also why adherent cells, the main constituent of living organisms, have not been explored. One method, femtosecond-resolved fluorescence spectroscopy, has recently elucidated the picosecond dynamics of water at a distance of  $\sim 7$  Å from a protein surface.<sup>10</sup> Although this technique is potentially available to monitor the global hydration state of various liq-

uid samples, it requires fluorescent preprocessing and is of no practical value to *in vivo* cell observations.

In this study, we propose a method to investigate intracellular water dynamics of the monolayer of cultured living cells by applying an emerging technology; terahertz time-domain attenuated total reflection (THz TD-ATR) spectroscopy.<sup>11</sup> With the advent of THz TD-ATR spectroscopy, observations of the picosecond dynamics of liquid water have been rapidly accelerated.<sup>12,13</sup> As mentioned by Arikawa *et al.*, the complex dielectric constant in the THz region provides useful information to directly evaluate the picosecond dynamics of hydration.<sup>12</sup> This is because the real part and imaginary part of the complex dielectric constant, which describe dielectric properties on a picosecond timescale,<sup>14</sup> can be determined using this methodology. Moreover, the penetration depth (i.e., evanescent wave: see explanation below) in this setup is of a magnitude of tens of micrometers. A common cell monolayer is several micrometers thick, so the sampled field in the evanescent wave of THz TD-ATR spectroscopy will encompass the whole cell monolayer. This cannot be possible in mid-infrared ATR spectroscopy, since the penetration depth in this region covers less than 1  $\mu\text{m}$  and only partial information of the cell monolayer is obtained.<sup>15</sup> Thus, THz TD-ATR spectroscopy is a prospective tool to evaluate intracellular hydration states on a picosecond timescale, not accessible by conventional methods and molecular dynamics (MD) simulations.

THz time-domain spectroscopy (THz-TDS) in transmission geometry has been widely applied to measure the physical properties of a sample by comparing temporal THz fields with and without the sample. From this technique, phase and intensity spectra are obtained, providing both real and imaginary parts of the complex dielectric constant.<sup>16</sup> However, it is extremely difficult to apply THz-TDS in transmission geometry to aqueous samples, because liquid water has a strong absorption in the THz region. Thus, a THz-TDS system using a reflection geometry has been pursued to determine the complex dielectric constant of aqueous samples.<sup>17,18</sup> Hirori *et al.* proposed that THz TD-ATR spectroscopy could be used for accurate determination of the complex dielectric constant of water.<sup>11</sup> This is because the temporal profile of the THz field

<sup>a)</sup>ogawayu@kais.kyoto-u.ac.jp.

measured with an ATR geometry provides information on the interaction between the sample and the evanescent wave. The ATR technique allowed us to better characterize strongly absorptive samples compared to a transmission and reflection geometry.<sup>19</sup> In THz TD-ATR spectroscopy, Fresnel's reflection coefficient of the prism-sample interface ( $\tilde{r}_{12}$ ) can be experimentally calculated from the Fourier transformed THz spectra of both reflectance ( $\tilde{R}$ ), and phase spectrum ( $\tilde{\Phi}$ ) in the frequency domain, as indicated below:<sup>20</sup>

$$\tilde{R} = \left| \frac{\tilde{r}_{12}}{r_{REF}} \right|^2, \quad (1)$$

$$\tilde{\Phi} = \text{Arg} \left[ \frac{\tilde{r}_{12}}{r_{REF}} \right], \quad (2)$$

where  $r_{REF}$  is the reflection coefficient of the prism-air interface. Additionally, the theoretical Fresnel's reflection coefficient of the prism-sample interface ( $\tilde{r}_{12}$ ) is expressed as a function of the incident angle ( $\theta$ ), and the (complex) dielectric constant of the ATR prism ( $\epsilon_1$ ) and the sample ( $\tilde{\epsilon}_2$ ).

$$\tilde{r}_{12} = \frac{\sqrt{\epsilon_1} \sqrt{1 - \left(\frac{\epsilon_1}{\tilde{\epsilon}_2}\right) \sin^2 \theta} - \sqrt{\tilde{\epsilon}_2} \cos \theta}{\sqrt{\epsilon_1} \sqrt{1 - \left(\frac{\epsilon_1}{\tilde{\epsilon}_2}\right) \sin^2 \theta} + \sqrt{\tilde{\epsilon}_2} \cos \theta}. \quad (3)$$

The solution of these simultaneous equations (1)–(3) determines the complex dielectric constant of the sample ( $\tilde{\epsilon}_2$ ), if other parameters are given.<sup>20</sup>

As illustrated in Fig. 1, in the case of a two-interface model for a bulk sample ( $\tilde{\epsilon}_3$ ) deposited on a thin layer ( $\tilde{\epsilon}_2$ ), the reflection coefficient of the layer-bulk interface ( $\tilde{r}_{23}$ ), as expressed by Eq. (4), needs to be taken into account, as well as the reflection coefficient of the prism-layer boundary ( $\tilde{r}_{12}$ ). When the thickness of the layer sample,  $d$ , is constant and a plane wave approximation is satisfied, the reflection coefficient  $\tilde{r}_{123}$  is described by Eq. (5).<sup>21</sup> Given  $\epsilon_1$ ,  $\tilde{\epsilon}_3$ ,  $\theta$ , and  $d$  are known parameters, the complex dielectric constant of the layer sample ( $\tilde{\epsilon}_2$ ) can be calculated by the same calculation process noted above.

$$\tilde{r}_{23} = \frac{\sqrt{\tilde{\epsilon}_2} \sqrt{1 - \left(\frac{\tilde{\epsilon}_2}{\tilde{\epsilon}_3}\right) \sin^2 \theta} - \sqrt{\tilde{\epsilon}_3} \sqrt{1 - \left(\frac{\tilde{\epsilon}_2}{\tilde{\epsilon}_3}\right) \sin^2 \theta}}{\sqrt{\tilde{\epsilon}_2} \sqrt{1 - \left(\frac{\tilde{\epsilon}_2}{\tilde{\epsilon}_3}\right) \sin^2 \theta} + \sqrt{\tilde{\epsilon}_3} \sqrt{1 - \left(\frac{\tilde{\epsilon}_2}{\tilde{\epsilon}_3}\right) \sin^2 \theta}}, \quad (4)$$

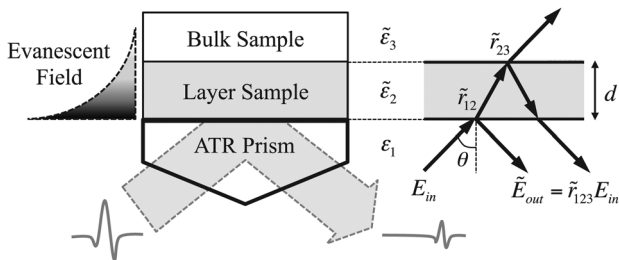


FIG. 1. Schematic illustration of THz TD-ATR spectroscopy with a two-interface model. Dielectric constants of the ATR prism, layer sample, and bulk sample are  $\epsilon_1$ ,  $\tilde{\epsilon}_2$ , and  $\tilde{\epsilon}_3$ , respectively. In addition to the reflection at the prism-layer boundary ( $\tilde{r}_{12}$ ), reflection at the layer-bulk boundary ( $\tilde{r}_{23}$ ) needs to be taken into account.

$$\tilde{r}_{123} = \frac{\tilde{r}_{12} + \tilde{r}_{23} \exp \left[ i \frac{4\pi d}{\lambda} \sqrt{\epsilon_1 \sin^2 \theta - \tilde{\epsilon}_2} \right]}{1 + \tilde{r}_{12} \tilde{r}_{23} \exp \left[ i \frac{4\pi d}{\lambda} \sqrt{\epsilon_1 \sin^2 \theta - \tilde{\epsilon}_2} \right]}. \quad (5)$$

To prove the validity of Eq. (5) for THz TD-ATR spectroscopy, we prepared an adhesive film as the sample layer with distilled water as a bulk sample on top of it. This preliminary experiment was performed using a TAS7500 (ADVANTEST Co.) with an ATR prism made of Si crystal that was equipped with a temperature controller. We directly attached the silicone adhesive film, having a thickness of 40  $\mu\text{m}$  (Kajixx Co., Ltd.), to the ATR prism and distilled water placed on top of the film. Using measurements of this silicone film and distilled water, we calculated the complex dielectric constant of the silicone film ( $\tilde{\epsilon}_2^{\text{Cal.}}$ ) according to Eq. (5). Among other parameters in Eq. (5), the dielectric constant value of the ATR prism ( $\epsilon_1$ ) was the same as that used in a previous study,<sup>22</sup> and distilled water ( $\tilde{\epsilon}_3$ ) was measured directly by THz TD-ATR spectroscopy. Additionally, we attached an 80  $\mu\text{m}$  silicone adhesive film (with the same composition as the 40  $\mu\text{m}$  silicone film) to the ATR prism to experimentally determine the complex dielectric constant of the silicone film alone ( $\tilde{\epsilon}_2^{\text{Mea.}}$ ) for comparison. All the measurements were performed from 0.3 to 3.0 THz while the prism was maintained at 25  $^\circ\text{C}$ .

All the measured complex dielectric constants are summarized in Fig. 2. Both the real and imaginary parts of distilled water showed a monotonic decrease with increase in frequency. This is because this frequency region is at the upper frequency limit for observing the slow Debye relaxation of water.<sup>12,13</sup> The slight presence of water was confirmed in the complex dielectric constant in the silicone film/distilled water sample below 0.8 THz. This is because the

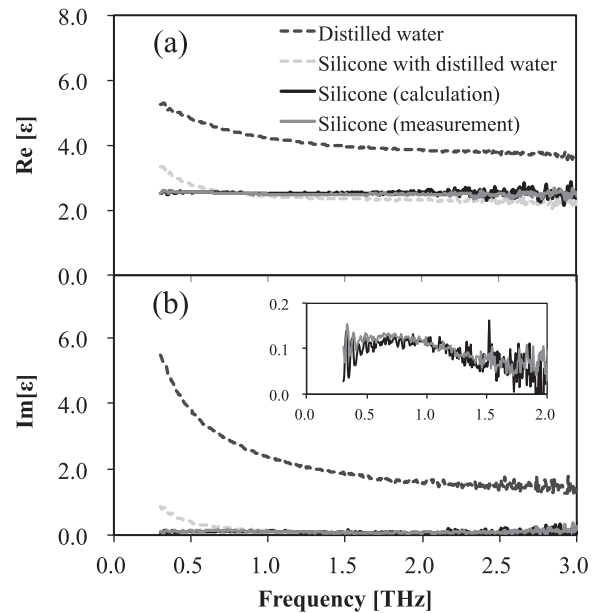


FIG. 2. (a) Real part and (b) imaginary part of the  $\tilde{\epsilon}_2^{\text{Cal.}}$  (black solid line) and  $\tilde{\epsilon}_2^{\text{Mea.}}$  (gray solid line). The  $\tilde{\epsilon}_2^{\text{Cal.}}$  was determined from the complex dielectric constant of the silicone film with distilled water (light gray broken line) and of distilled water (dark gray broken line). The  $\tilde{\epsilon}_2^{\text{Cal.}}$  had a good agreement with  $\tilde{\epsilon}_2^{\text{Mea.}}$ , which proved the validity of Eq. (5) in THz TD-ATR spectroscopy. The inset shows the close-up of the imaginary part of  $\tilde{\epsilon}_2^{\text{Cal.}}$  and  $\tilde{\epsilon}_2^{\text{Mea.}}$ .

depth of penetration of the evanescent field into the sample is beyond  $40\ \mu\text{m}$  in this case. On the other hand, the  $\tilde{\epsilon}_2^{\text{Cal.}}$  does not have the distinctive spectral features of distilled water, indicating the results derived from Eq. (5) were free from the contribution of distilled water. In fact,  $\tilde{\epsilon}_2^{\text{Mea.}}$  was in good agreement with  $\tilde{\epsilon}_2^{\text{Cal.}}$  for both the real and imaginary parts. From these preliminary experimental results, we concluded that Eq. (5) is able to determine the complex dielectric constant of the sample layer when THz TD-ATR spectroscopy is used.

In the next phase of the experiment, we directly attached a cell incubation chamber onto the ATR prism in order to culture the cells. The top of the incubation chamber was a transparent window, so the cell growth could be monitored using a digital microscope (KEYENCE Co., VH-Z50L) mounted just above the cell incubator. Intestinal epithelial cancer cell, DLD-1, was cultured with a RPMI-1640 medium (Wako Pure Chemical Industries, Ltd.) at  $37^\circ$  in a humidified atmosphere of 5%  $\text{CO}_2$  in the incubation chamber. The medium is a dilute solution with minute amounts of various inorganic salts, amino acids, and vitamins. To remove excess suspended cells, the medium was renewed in the middle of cell incubation. After 72 h, it was observed that the ATR prism was completely covered with a DLD-1 cell monolayer. THz TD-ATR measurements were then performed with the ATR prism maintained at  $37^\circ$ . In this case, the prism-cell-medium boundary is considered to be a two-interface model and Eq. (5) was applied to eliminate the contribution of the bulk medium above the DLD-1 cell monolayer. Here, we assume that the cell monolayer has a flat surface that satisfies a plane wave approximation. Observation of fluorescently stained DLD-1 monolayer on a glass plate using a confocal fluorescent microscope (Nikon Co., A-1) revealed that the thickness of the cell monolayer ( $d$ ) was  $6.5 \pm 1.0\ \mu\text{m}$ . For comparison, the complex dielectric constant of the medium alone was measured under the same conditions.

The calculated complex dielectric constant of the DLD-1 cell monolayer is compared with that of the medium alone in Fig. 3. The chemical composition of the medium was so dilute that the complex dielectric constant of medium alone was not significantly different from that of pure distilled water at the same temperature. Between 0.3 and 3.0 THz, the complex dielectric constant of water is decomposed into three components: the slow Debye relaxation mode, the fast Debye relaxation mode, and the intermolecular vibration mode.<sup>13</sup> Among them, the slow relaxation mode is very sensitive to hydration in the THz region measured, while the fast relaxation mode and the intermolecular vibration mode were not affected to any great degree by hydration.<sup>23</sup> Given that the imaginary part in the lower frequency region is dominated by the slow relaxation mode; the decreased imaginary part of the cell monolayer in Fig. 3(b) was interpreted as a significant hydration effect. From this point of view, this result indicates a highly developed intracellular hydration condition. This seems to contradict the previous NMR or QENS measurements, which have revealed that more than 80% of intracellular water molecules have bulk-like dynamics.<sup>8,9</sup> In those methods, only strongly perturbed water molecules with sub-nanosecond dynamics are defined as hydrated water, while in THz spectroscopy water molecules weakly

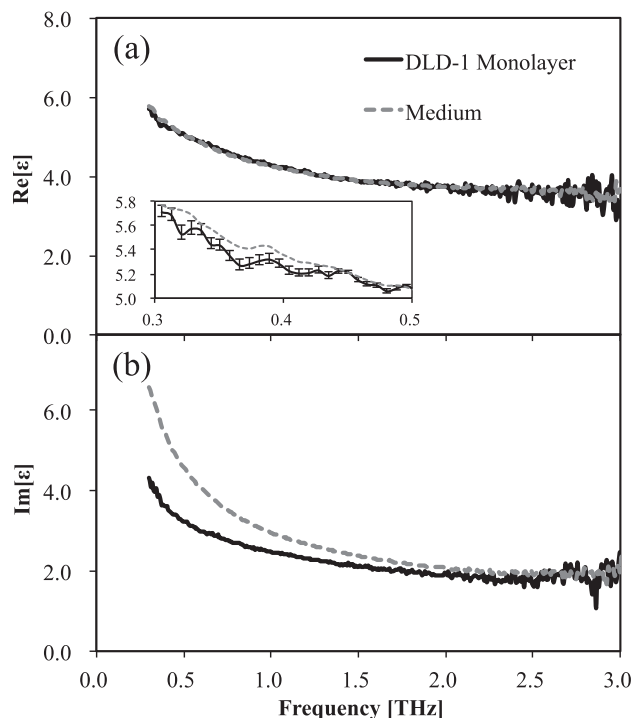


FIG. 3. (a) Real part and (b) imaginary part of the complex dielectric constant of DLD-1 monolayer (black solid line) and medium (gray broken line) at  $37^\circ$ . The inset shows the close-up of the real part between 0.3 and 0.5 THz and the error bar derives from fluctuation of the thickness of DLD-1 ( $6.5 \pm 1.0\ \mu\text{m}$ ) estimated by confocal fluorescent microscopic three-dimensional images.

bonded to biological macromolecules are likely to be regarded as hydration water, and thus a global hydration state was observed in the current experiment. On the other hand, only a slight decrease of the real part of the complex dielectric constant of cell monolayer below 0.5 THz was observed. We fitted our result in accordance with Yada *et al.*<sup>24</sup> This showed that the slow relaxation mode in the real part of DLD-1 monolayer occupies only 2% of the total dielectric constant at 0.5 THz, while the contribution of the slow relaxation in the imaginary part reaches 64%. This was thought to be because over 90% of the real part of distilled water is dominated by high-frequency vibration resonance (i.e., intermolecular vibration modes, intramolecular vibration modes, and electron excitations), which has much less sensitivity to hydration in this region.<sup>23</sup>

Our results performed by THz TD-ATR spectroscopy have similar tendency to the previous studies that showed the complex refractive index of *ex vivo* cancer cell tissues measured by THz-TDS in transmission geometry.<sup>25,26</sup> In those studies, cell tissues ( $\sim 500\ \mu\text{m}$ ) were excised from patients and placed in a holder between two 1 mm thick quartz windows to obtain the transmitted THz pulse with high accuracy. However, the sliced tissues are apt to be denaturalized in the waterless condition. Furthermore, the fact that the cancer cells and normal cells in the sliced tissues are not uniformly distributed makes it difficult to discuss the THz response in detail. On the other hand, THz TD-ATR spectroscopy assures *in vivo* measurement of cell monolayer in liquid medium, which allowed us to determine the dielectric properties of cells in similar circumstances inside the biological body.



To conclude, we demonstrated that THz TD-ATR spectroscopy coupled with a two-interface (prism-cell layer-bulk medium) calculation model is a powerful investigative technique. Results from preliminary experiments were used to remove the contribution of distilled water (bulk sample) to determine the calculated complex dielectric constant of the silicone film ( $\tilde{\epsilon}_2^{\text{Cal.}}$ ). Our calculation successfully reproduced the measured result ( $\tilde{\epsilon}_2^{\text{Mea.}}$ ), which confirms the validity of Eq. (5). This calculation was also demonstrated to determine the complex dielectric constant of the DLD-1 cell monolayer, assuming the cell monolayer is a flat surface. The obtained imaginary part suggests a well-developed hydration state with a picosecond timescale inside cells. This result seemingly conflicts with NMR and QENS measurements, but in fact because THz spectroscopy evaluates the global hydration state rather than just those water molecules directly bonded to the biomolecule, our results provide a perspective of intracellular water dynamics.

We are grateful to Professor Koichiro Tanaka and Dr. Tomoko Tanaka (iCeMS, Kyoto University, Japan) for their technical supports and useful discussions. We thank Mr. Takafumi Kajitani (Kajixx Co., Ltd.) for providing us the silicone film and Professor Garry John Piller (Graduate School of Agriculture, Kyoto University, Japan) for his constructive suggestions. Financial support was provided by Industry-Academia Collaborative R&D from Japan Science and Technology Agency (JST).

<sup>1</sup>B. N. G. Giepmans, S. R. Adams, M. H. Ellisman, and R. Y. Tsien, *Science* **312**, 217 (2006).

<sup>2</sup>N. Nandi and B. Bagchi, *J. Phys. Chem. B.* **101**, 10954 (1997).

- <sup>3</sup>S. K. Sinha, S. Chakraborty, and S. Bandyopadhyay, *J. Phys. Chem. B* **112**, 8203 (2008).
- <sup>4</sup>M. Chaplin, *Nat. Rev. Mol. Cell Biol.* **7**, 861 (2006).
- <sup>5</sup>K. Asami, T. Yonezawa, H. Wakamatsu, and N. Koyanagi, *Bioelectrochem. Bioenerg.* **40**, 141 (1996).
- <sup>6</sup>J. Qvist, E. Persson, C. Mattea, and B. Halle, *Faraday Discuss.* **141**, 131 (2009).
- <sup>7</sup>M. Tehei, B. Franzetti, K. Wood, F. Gabel, E. Fabiani, M. Jasnin, M. Zamponi, D. Oesterhelt, G. Zaccai, M. Ginzburg, and B.-Z. Ginzburg, *Proc. Natl. Acad. Sci. USA* **104**, 766 (2007).
- <sup>8</sup>P. Ball, *Chem. Phys. Chem.* **9**, 2677 (2008).
- <sup>9</sup>D. M. Leitner, M. Gruebele, and M. Havenith, *HFSP J.* **2**, 314 (2008).
- <sup>10</sup>S. K. Pal, J. Peon, and A. H. Zewail, *Proc. Natl. Acad. Sci. USA* **99**, 1763 (2002).
- <sup>11</sup>H. Hirori, K. Yamashita, M. Nagai, and K. Tanaka, *Jpn. J. Appl. Phys., Part 2* **43**, L1287 (2004).
- <sup>12</sup>T. Arikawa, M. Nagai, and K. Tanaka, *Chem. Phys. Lett.* **457**, 12 (2008).
- <sup>13</sup>H. Yada, M. Nagai, and K. Tanaka, *Chem. Phys. Lett.* **464**, 166 (2008).
- <sup>14</sup>A. G. Markelz, *IEEE J. Sel. Top. Quantum Electron.* **14**, 180 (2008).
- <sup>15</sup>K. Miyamoto, P. Yamada, R. Yamaguchi, T. Muto, A. Hirano, Y. Kimura, M. Niwano, and H. Isoda, *Cytotechnology* **55**, 143 (2007).
- <sup>16</sup>S. W. Smye, J. M. Chamberlain, A. J. Fitzgerald, and E. Berry, *Phys. Med. Biol.* **46**, 101 (2001).
- <sup>17</sup>C. Rønne, P. O. Åstrand, and S. R. Keiding, *Phys. Rev. Lett.* **82**, 2888 (1999).
- <sup>18</sup>U. Møller, D. G. Cooke, K. Tanaka, and P. U. Jepsen, *J. Opt. Soc. Am. B* **26**, A113 (2009).
- <sup>19</sup>P. U. Jepsen, D. G. Cooke, and M. Koch, *Laser Photonics Rev.* **5**, 124 (2011).
- <sup>20</sup>M. Nagai, H. Yada, T. Arikawa, and K. Tanaka, *Int. J. Infrared Millim. Waves* **27**, 505 (2006).
- <sup>21</sup>J. D. E. McIntyre and D. E. Aspnes, *Surf. Sci.* **24**, 417 (1971).
- <sup>22</sup>J. Dai, J. Zhang, W. Zhang, and D. Grischkowsky, *J. Opt. Soc. Am. B.* **21**, 1379 (2004).
- <sup>23</sup>M. Hishida and K. Tanaka, *J. Phys. Condens. Matter* **24**, 284113 (2012).
- <sup>24</sup>H. Yada, M. Nagai, and K. Tanaka, *Chem. Phys. Lett.* **473**, 279 (2009).
- <sup>25</sup>V. P. Wallace, A. J. Fitzgerald, E. Pickwell, R. J. Pye, P. F. Taday, N. Flanagan, and T. Ha, *Appl. Spectrosc.* **60**, 1127 (2006).
- <sup>26</sup>P. C. Ashworth, E. Pickwell, E. Provenzano, S. E. Pinder, A. D. Purushotham, M. Pepper, and V. P. Wallace, *Opt. Express* **17**, 12444 (2009).